

Evaluating the Importance of Long-Range Interactions in the Thermodynamic Description of the Choline Chloride/Water System

Ahmad Alhadid, Mirjana Minceva, João A. P. Coutinho, and Simão P. Pinho*



Cite This: <https://doi.org/10.1021/acs.iecr.5c04412>



Read Online

ACCESS |



Metrics & More

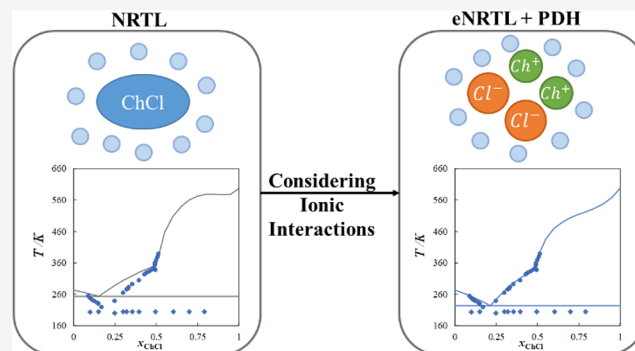


Article Recommendations



Supporting Information

ABSTRACT: The ability to model salt-containing deep eutectic solvents (DES) is essential for their rational design and application. Most existing thermodynamic models treat salts as neutral species, neglecting ionic interactions. This work investigates the explicit inclusion of ionic effects in modeling the liquid-phase nonideality of the binary choline chloride (ChCl)/water system. Experimental vapor–liquid equilibrium, solid–liquid equilibrium, water activity, and ChCl activity coefficients obtained from isopiestic measurements were used. Short-range molecular interactions were described with the nonrandom two-liquid (NRTL) model, while long-range ionic interactions were incorporated through the Pitzer–Debye–Hückel (PDH) term. Treating ChCl as a fully dissociated electrolyte and including the PDH contribution significantly improved the representation of nonideality across low and high salt concentrations. These results demonstrate the importance of electrolyte-based modeling frameworks for the development, optimization, and recycling of water-containing DES Types II–IV.



1. INTRODUCTION

Eutectic mixtures with a large depression in the melting temperature have emerged as a new class of designer solvents under the name deep eutectic solvents (DES).^{1,2} The key to designing DES lies in selecting ionic plastic crystalline materials, which possess low melting enthalpy and entropy and can induce significant negative deviations from ideality when mixed with hydrogen bond donors.^{3–6}

Modeling the liquid-phase nonideality of DES and their mixtures is essential for accurately describing their phase behavior and performance.^{7,8} This requires knowledge of the activity coefficients of the components in the liquid phase, which can be calculated by using either predictive or correlative thermodynamic models. Various activity coefficient models have been employed in the literature to capture the nonideal behavior of DES, including COSMO-based models,^{9–14} UNIFAC,^{15–17} NRTL,^{18,8} PC-SAFT,^{19–22} and Redlich–Kister expansions.^{8,23,24} The binary interaction parameters of correlative models are typically estimated by using vapor–liquid (VLE), liquid–liquid (LLE), or solid–liquid equilibrium (SLE) data. However, only a few studies have considered the simultaneous modeling of VLE, LLE, and SLE data using the same set of model parameters to ensure that the models accurately describe the nonideality of the solution rather than simply partially correlating the phase equilibria data.^{20,21,25–27}

The importance of describing the ionic interactions in DES has been addressed in the literature.^{9,13,24} Although one could

argue that ion pairs, instead of dissociated ions, are dominant in organic salt–organic compound solutions, DES are often used with large water concentrations to enhance their properties and performance. Hence, the importance of dissociated ions in these systems and their interactions should be considered. When electrolyte solutions are modeled, cations and anions are treated as separate species in the liquid phase; therefore, the binary salt/solvent solution is modeled as a ternary cation/anion/solvent mixture. The activity coefficients of components can be calculated by summing the contributions arising from short- and long-range interactions. The contribution to the activity coefficients arising from the short-range interactions can be calculated using common excess Gibbs energy models, such as NRTL or COSMO-RS, while the contribution to the activity coefficients arising from the long-range interactions can be calculated using Debye–Hückel-based terms, such as the extended Debye–Hückel or the Pitzer–Debye–Hückel (PDH).^{28,29} DES were modeled as electrolyte solutions where the salt was assumed to fully dissociate as cations and anions in the liquid phase using

Received: October 23, 2025

Revised: February 10, 2026

Accepted: February 12, 2026

COSMO-RS^{9,11} and COSMO-SAC.¹³ However, only short-range interactions were considered. One reason that hinders modeling the long-range interactions in DES is the lack of experimental data to describe the long-range interactions, namely, the density and permittivity of the mixture. It is a fact that assumptions such as a fixed dielectric medium and density, as well as a limited treatment of the existing interactions, reduce the accuracy of the physical-chemistry description of the systems at high concentrations and in low-permittivity or nonaqueous systems.^{30–33} As a result, several alternatives and extensions have been developed, including extended or modified PDH expressions^{30–32} with concentration-dependent properties and considering different degrees of dissociation.³³ The PDH term is therefore often used as a baseline long-range term, which can be complemented by these advanced approaches to ensure higher consistency; however, this cannot be guaranteed in the very important mixture studied in this work, because it spans the entire composition range and temperature from 204 to 687 K, which brings out the impossibility of correctly describing the density and permittivity of the mixture depending on the temperature and composition. Nevertheless, electrolyte-based thermodynamic frameworks are essential for modeling water-containing DES Types II–IV because water promotes ionic dissociation, making long-range electrostatic interactions a crucial driving force for nonideality,³⁴ which cannot be captured by molecular activity coefficient models alone.

Choline chloride (ChCl)/water is a binary eutectic mixture showing a strong negative deviation from ideality and a large depression in the melting temperature of the mixture at the eutectic point ($T_e \approx 204$ K),³⁵ which has been proposed to act as a DES or low transition-temperature mixture (LTTM).^{36,37} For water, the density and permittivity over a wide temperature range are available in the literature.^{38,39} Phase equilibria data and activity coefficients of ChCl and water in the ChCl/water mixture are also available in the literature. For instance, the activity coefficients of ChCl at 298.15 K were measured by the isopiestic method in three different studies.^{40–42} Additionally, the water activity in the ChCl/water mixture at 298.15 and 313.15 K was measured by a vapor pressure osmometer.^{43,44} Lobo Ferreira et al.³⁵ reported the SLE phase diagram of ChCl/water. Moreover, the bubble point of the ChCl/water mixture in the temperature range 303.1 to 410 K and pressure range 2–100 kPa was studied in the literature.^{26,45,46} Van den Bruinhorst et al.⁴⁷ reported the heat of mixing in the ChCl/water mixture. Thus, ChCl/water represents a model salt-based eutectic mixture that can be used to study the influence of ionic interactions on the modeling of nonideality in these mixtures, generally called DES.

This work studies the description of the liquid phase nonideality in ChCl/water, considering the ionic interactions and assuming ChCl as associated or fully dissociated ions. Phase equilibria data published in the literature were used to fit the binary interaction parameters of the NRTL model to describe the short-range interactions. The PDH term was employed to model long-range interactions. The study aims to provide insights into the importance of modeling ionic interactions in describing the phase behavior of salt-based eutectic mixtures.

2. MATERIALS AND METHODS

2.1. Activity Coefficients and Modeling

In its most general form, in this work, the rational symmetric activity coefficients of component i (γ_i) were considered to be the sum of the short-range (γ_i^{SR}) and long-range (γ_i^{LR}) contributions:

$$\ln \gamma_i = \ln \gamma_i^{SR} + \ln \gamma_i^{LR} \quad (1)$$

The short-range contribution was calculated using the NRTL:²⁸

$$\ln \gamma_i^{SR} = \frac{\sum_{j=1}^m \tau_{ji} G_{ji} x_j}{\sum_{l=1}^m G_{li} x_l} + \sum_{j=1}^m \frac{x_j G_{ij}}{\sum_{l=1}^m G_{lj} x_l} \left(\tau_{ij} - \frac{\sum_{r=1}^m \tau_{rj} G_{rj} x_r}{\sum_{l=1}^m G_{lj} x_l} \right) \quad (2)$$

$$G_{ij} = \exp(-\alpha_{ij} \tau_{ij}) \quad \text{with } \alpha_{ij} = \alpha_{ji} \quad (3)$$

$$\tau_{ij} = \frac{A_{ij}}{RT} \quad (4)$$

where A_{ij} and A_{ji} are the binary interaction parameters between species i and j , and α_{ij} is the nonrandomness parameter.

In the assumption of fully dissociated ions, the cholinium cation and chloride anion are considered separate species in the liquid phase. The mole fraction of any ion species (k) was calculated as follows:

$$x_k^{\text{ternary}} = \frac{x_i^{\text{binary}}}{1 + x_{\text{ChCl}}^{\text{binary}}} \quad (5)$$

where x_k^{ternary} is the mole fraction of ion k in the ternary cholinium/chloride/water solution and x_i^{binary} its corresponding mole fraction of ChCl or water in the binary ChCl/water solution. Considering dissociation, the rational symmetric activity coefficients of the ions are initially calculated, while the corresponding activity coefficient of ChCl is obtained by the mean ionic activity coefficient calculated by

$$\ln \gamma_{\pm}^{SR} = \frac{1}{2} (\ln \gamma_+^{SR} + \ln \gamma_-^{SR}) \quad (6)$$

where subscripts (\pm), (+), and (−) represent the salt, cation, and anion, respectively. In the symmetric convention, the reference state is the pure liquid at the system pressure and temperature. When considering ion dissociation, ChCl is an equimolar mixture of cholinium and chloride. Thus, the short-range contribution for the salt activity coefficient is complete when rewriting eq 6 to

$$\ln \gamma_{\pm}^{SR}(x, T) = \frac{1}{2} (\ln \gamma_+^{SR}(x, T) + \ln \gamma_-^{SR}(x, T)) - \frac{1}{2} (\ln \gamma_+^{SR}(0.5, T) + \ln \gamma_-^{SR}(0.5, T)) \quad (7)$$

The long-range contribution was calculated using the PDH term as follows²⁹

$$\ln \gamma_i^{LR} = - \left(\frac{1000}{M} \right)^{1/2} A_{\phi} \left\{ (2z_i^2/b) \ln(1 + bI_x^{1/2}) + \frac{(z_i^2 I_x^{1/2} - 2I_x^{3/2})}{(1 + bI_x^{1/2})} \right\} \quad (8)$$

where M is the molecular weight of water; A_{ϕ} is the Debye–Hückel parameter, which depends on the temperature; z_i is the species charge; b is the closest approach parameter, generally a fixed value of 14.9;²⁹ and I_x is the ionic strength on a mole fraction basis. The Debye–Hückel parameter (A_{ϕ}) and the ionic strength on a mole fraction basis (I_x) were calculated as follows:

$$A_{\phi} = (1/3) \left(\frac{2\pi N_A \rho}{1000} \right)^{1/2} \left(\frac{e^2}{4\pi \epsilon_0 \epsilon_r kT} \right)^{3/2} \quad (9)$$

Table 1. Transition Properties of Pure Components Considered in This Work

Component		$\Delta h_{fus}/\text{kJ mol}^{-1}$	T_{fus}/K	$\Delta_{fus}c_p/\text{J mol}^{-1} \text{K}^{-1}$	$\Delta h_{tr,i}/\text{kJ mol}^{-1}$	T_{tr}/K	$\Delta_{tr}c_p/\text{J mol}^{-1} \text{K}^{-1}$
Choline chloride	Set 1	13.8 ³	687 ³	20.3 ⁴⁷	17.3 ³⁵	340 ³⁵	20.0 ^{35,47}
	Set 2	4.3 ⁴⁹	597 ⁴⁹	0	17.3 ³⁵	340 ³⁵	20.0 ^{35,47}
Water		6.01 ⁵¹	273.1 ⁵¹	37.94 ⁵¹	–	–	–

$$I_x = \frac{1}{2} \sum z_i^2 x_i \quad (10)$$

where N_A is Avogadro's constant; ρ is the density of the solvent; e is the electron charge; ϵ_0 is the vacuum permittivity; ϵ_r is the dielectric constant of the solvent; k is Boltzmann's constant; T is the absolute temperature. The Debye–Hückel parameter (A_ϕ) depends on density, permittivity, and temperature. Moreover, density and permittivity are also functions of temperature. Clarke and Glew³⁹ evaluated the water Debye–Hückel parameter from 273.15 to 423.15 K, representing its temperature dependence using a general thermodynamic expression. A linear temperature dependence ($R^2 = 0.9803$) was used to decrease the complexity of calculations at different temperatures (see Figure S1 in the Electronic Supporting Information (ESI) file).

ChCl is a 1:1 salt, and by rearranging eq 8, the long-range contribution to the mean rational activity coefficient of ChCl (γ_{\pm}^{LR}) can be calculated as follows:²⁹

$$\ln \gamma_{\pm}^{LR} = -\left(\frac{500}{M}\right)^{1/2} A_\phi \left\{ (2^{3/2}/b) \ln \left(\frac{1 + 2^{-1/2} b x_2^{1/2}}{1 + 2^{-1/2} b} \right) + \frac{(x_2^{1/2} - x_2^{3/2})}{(1 + 2^{-1/2} b x_2^{1/2})} \right\} \quad (11)$$

where x_2 is the summation of cation and anion mole fractions. Water is a neutral species (i.e., $z = 0$). By rearranging eq 8, the long-range contribution to the activity coefficients of water was calculated as follows:

$$\ln \gamma_{water}^{LR} = \left(\frac{1000}{M}\right)^{1/2} A_\phi \left\{ \frac{(\frac{1}{2}x_2)^{3/2}}{(1 + b(\frac{1}{2}x_2)^{1/2})} \right\} \quad (12)$$

The isopiestic data report the molal unsymmetric activity coefficients (i.e., $\gamma_{\pm,unsymm}^m \rightarrow 1$ as $x_{ion} \rightarrow 0$). Therefore, two conversions are needed. First, unsymmetric rational activity coefficients ($\gamma_{\pm,unsymm}$) of ChCl were calculated from the symmetric mean activity coefficients using eqs 1, 2, 7, and 11 as follows:

$$\ln \gamma_{\pm,unsymm} = \ln \gamma_{\pm} - \ln \gamma_{\pm}^{\infty} \quad (13)$$

where γ_{\pm}^{∞} is the ChCl infinite dilution activity coefficient. In a second stage, the experimental molal unsymmetric activity coefficient ($\gamma_{\pm,unsymm}^m$) is converted to the rational activity coefficients ($\gamma_{\pm,unsymm}$) by

$$\gamma_{\pm,unsymm} = \frac{\gamma_{\pm,unsymm}^m}{x_{water}} \quad (14)$$

The partial molar excess enthalpy of water was calculated as follows:

$$\left(\frac{\partial \ln \gamma_{water}}{\partial T} \right)_{x,P} = -\frac{\bar{h}_{water}^E}{RT^2} \quad (15)$$

The activity coefficient of water at a specific mole fraction was calculated in the temperature range of 200 to 400 K. The calculated activity coefficients were fitted to a second-degree polynomial, and the partial molar enthalpy of water at the specific mole fraction and 298.1 K was calculated from the derivative of the polynomial as per eq 15.

2.2. VLE Calculations

The bubble point of the binary ChCl/water mixture was calculated assuming the ideality of the vapor phase and assuming ChCl to be completely nonvolatile:

$$P = x_{water} \gamma_{water} P_{water}^{sat} \quad (16)$$

where P is the total pressure and P_{water}^{sat} is the saturation pressure of water at the bubble-point temperature. The saturation pressure of water was calculated using the formula from Matsunaga and Nagashima⁴⁸ (see Table S1 in the ESI for details).

2.3. SLE Calculations

After some thermodynamic assumptions, the liquidus lines of water and ChCl were calculated as follows:

$$\ln x_i \gamma_i = \frac{\Delta h_{fus,i}}{RT} \left(\frac{T}{T_{fus,i}} - 1 \right) - \frac{\Delta_{fus}c_{p,i}}{R} \left(1 - \frac{T}{T_{fus,i}} + \ln \frac{T}{T_{fus,i}} \right) \quad (17)$$

where Δh_{fus} and T_{fus} are the melting enthalpy and temperature of the pure component i , and $\Delta_{fus}c_p$ is the difference between the heat capacity of the pure component in the solid and liquid states, estimated at its melting temperature. ChCl undergoes a solid–solid transition at around 340 K,³⁵ and its liquidus line below the solid–solid transition temperature was calculated as follows:

$$\ln x_i \gamma_i = \frac{\Delta h_{fus,i}}{RT} \left(\frac{T}{T_{fus,i}} - 1 \right) + \frac{\Delta h_{tr,i}}{RT} \left(\frac{T}{T_{tr,i}} - 1 \right) - \frac{\Delta_{fus}c_{p,i}}{R} \left(1 - \frac{T_{fus,i}}{T} + \ln \frac{T_{fus,i}}{T} \right) - \frac{\Delta_{tr}c_{p,i}}{R} \left(1 - \frac{T_{tr,i}}{T} + \ln \frac{T_{tr,i}}{T} \right) \quad (18)$$

where Δh_{tr} and T_{tr} are the solid–solid transition enthalpy and temperature of the pure component (i.e., ChCl), and $\Delta_{tr}c_p$ is the difference between the heat capacity of ChCl in the two different solid states, estimated at the solid–solid transition temperature.

ChCl is thermally unstable, and its melting properties are not well-defined. Two sets of melting properties of ChCl are commonly used in the literature. Fernandez et al.⁴⁹ provided an indirect estimate for the melting enthalpy and temperature of ChCl using the SLE data of binary ChCl/ionic liquid mixtures. On the other hand, van den Bruinhorst et al.³ directly measured the melting properties of ChCl utilizing fast-scanning calorimetry. Because the two sets are significantly different, both sets were considered in this work. Table 1 shows the melting properties used to represent the SLE phase diagram of ChCl/water.

When ChCl is assumed to be fully dissociated, the SLE phase diagram was modeled by assuming the following reaction:



The solubility constant (K_{SP}) was calculated as follows:⁵⁰

$$K_{SP} = \frac{1}{4} x_{ChCl}^2 \gamma_{\pm}^2 \quad (20)$$

The liquidus line above and below the solid–solid transition temperature of ChCl was calculated using the right-hand side of eqs 17 and 18, respectively.

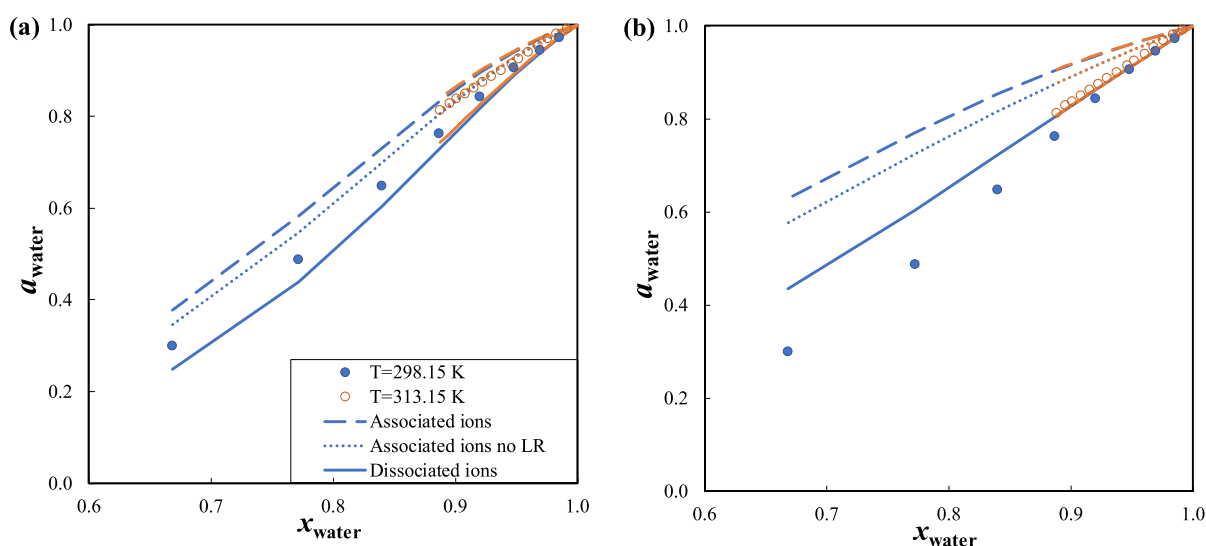


Figure 1. Water activity in choline chloride (ChCl)/water at 298.15 and 313.15 K modeled assuming different representations of ChCl and calculated using the binary interaction parameters obtained when considering the melting properties of ChCl reported by (a) van den Bruinhorst et al.³ or (b) Fernandez et al.⁴⁹ Experimental data were taken from refs.^{43,44}.

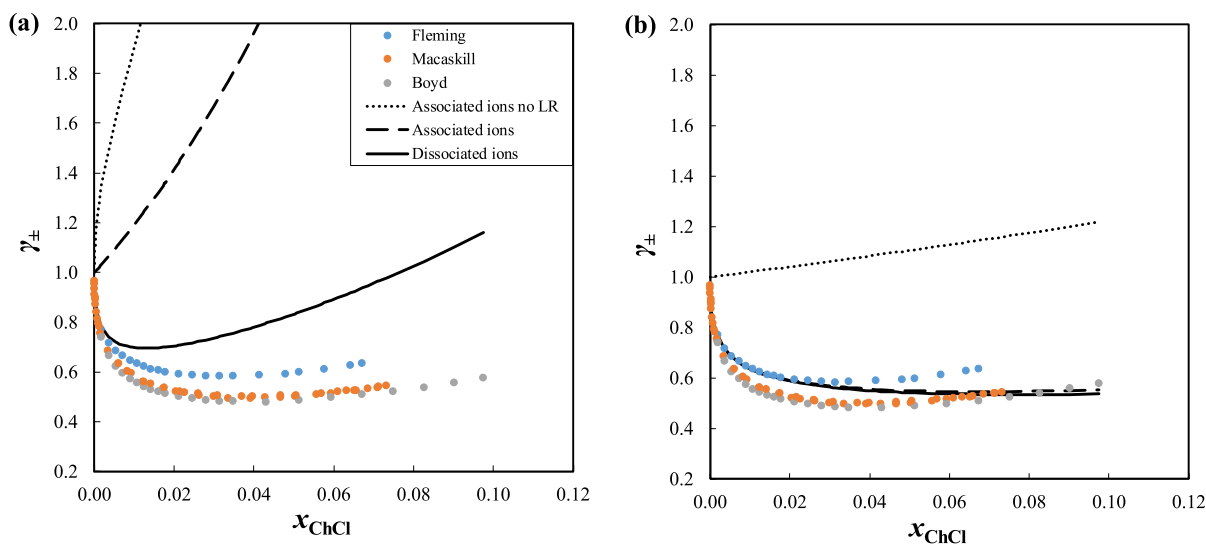


Figure 2. Mean activity coefficients of choline chloride (ChCl) in ChCl/water at 298.15 K modeled assuming different representations of ChCl, and calculated using the binary interaction parameters obtained when considering the melting properties of ChCl reported by (a) van den Bruinhorst et al.³ or (b) Fernandez et al.⁴⁹ Experimental data were taken from refs.^{40–42}.

2.3.1. Model Parameters Estimation. The NRTL model parameters in eqs 2–4 were estimated by fitting experimental VLE, SLE, water activity, and data from isopiestic measurements simultaneously. The nonrandomness parameter (α) was set to 0.3. In the case of VLE and activity coefficients of ChCl and water, the objective function is

$$OF1 = \sum \left(\frac{\gamma^{cal} - \gamma^{exp}}{\gamma^{exp}} \right)^2 \times 100 \quad (21)$$

where γ^{cal} and γ^{exp} are the calculated activity coefficients by eq 1 and experimental activity coefficients, respectively. To consider SLE data, the objective function was:

$$OF2 = \sum (T^{cal} - T^{exp})^2 \quad (22)$$

where T^{cal} and T^{exp} are the calculated and experimental liquidus temperatures, at a given experimental composition, respectively.

Three cases were considered when modeling ChCl, namely, associated ions with no long-range term, associated ions with a long-

range term, and fully dissociated ions with a long-range term. When choline chloride (ChCl) is assumed to exist as an associated ion, two binary interaction parameters are obtained. In contrast, assuming full dissociation of ChCl in the liquid phase results in six binary interaction parameters. The specific set of ChCl melting properties used also affects the resulting parameters. Table S2 in the ESI reports the NRTL parameters obtained for different molecular representations and melting properties of ChCl. Table S3 in the ESI reports the error weight for each data type in the objective function.

3. RESULTS AND DISCUSSION

3.1. Isopiestic and Water Activity

As shown in Table S2, depending on the selected thermodynamic framework and the different melting properties of ChCl, the obtained NRTL model binary interaction parameters change and, consequently, the calculated activity coefficients of both components. Figure 1 shows the activity coefficients of water in the ChCl/water system at 298.15 and

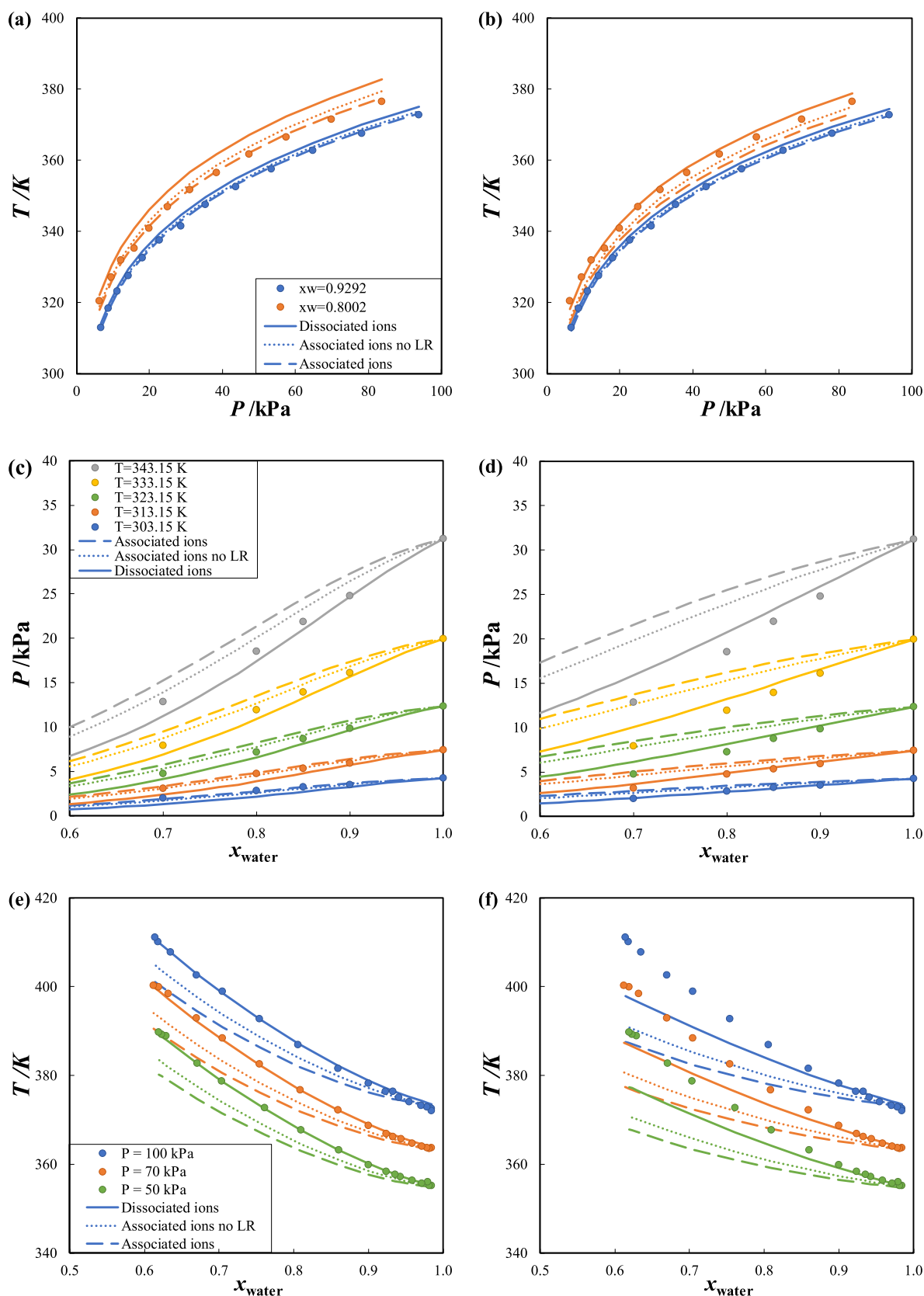


Figure 3. Vapor–liquid equilibrium in the choline chloride (ChCl)/water system modeled assuming different representations of ChCl and calculated using the binary interaction parameters obtained when considering the melting properties of ChCl reported in (a), (c), and (e) van den Bruinhorst et al.³ or (b), (d), and (f) Fernandez et al.⁴⁹ Experimental data were taken from refs.^{26,45,46}

313.15 K, modeled by assuming different representations of ChCl when using the binary interaction parameters obtained

considering ChCl melting properties Set 1 (Figure 1a) and Set 2 (Figure 1b). As seen in Figure 1a, the water activity at 298.15

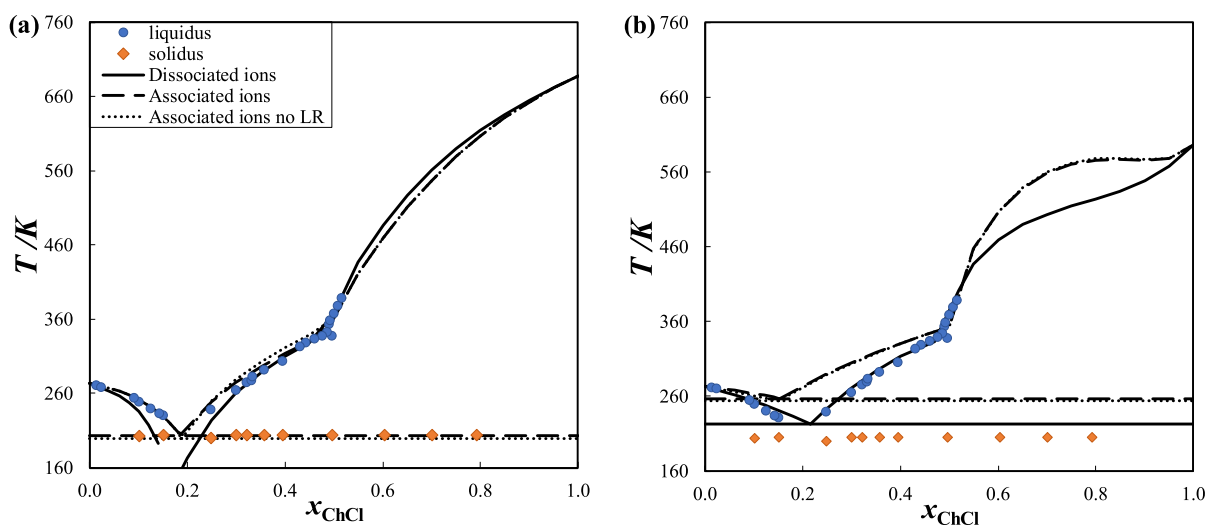


Figure 4. Solid–liquid equilibrium (SLE) in choline chloride (ChCl)/water modeled by assuming different representations of ChCl. SLE was calculated using the melting properties of ChCl reported in (a) van den Bruinhorst et al.³ or (b) Fernandez et al.⁴⁹ Experimental data were taken from refs. 19,35,36.

K is underestimated when assuming ChCl as dissociated ions (solid lines) and using the ChCl melting properties Set 1. In contrast, the water activity is slightly overestimated when assuming ChCl as associated ions with (dashed lines) and without (dotted lines) the long-range term. On the other hand, the water activity is consistently overestimated when using ChCl melting properties Set 2. Assuming ChCl as dissociated ions and using ChCl melting properties Set 2 allows for better correlation of water activity data at 298.15 and 313.15 K compared to assuming ChCl as associated ions.

Figure 2 shows the mean activity coefficient of ChCl in the ChCl/water system from isopiestic measurements and those modeled assuming different representations of ChCl when using the NRTL model binary interaction parameters obtained considering ChCl melting properties Set 1 (Figure 2a) and Set 2 (Figure 2b). The mean activity coefficients reported by Fleming⁴⁰ are slightly larger than those measured by Macaskill et al.⁴¹ and Boyd et al.⁴² As seen in Figure 2, modeling ChCl mean activity coefficients is possible only when considering the long-range interaction term. When using ChCl melting properties Set 1 (Figure 2a), the mean activity coefficients of ChCl are overestimated. Nevertheless, when ChCl is assumed to be dissociated ions, a good qualitative description can be observed. On the other hand, the mean activity coefficients of ChCl can be well-described when using ChCl melting properties Set 2 (Figure 2b), whether considering ChCl as dissociated or associated ions. In conclusion, modeling ChCl as dissociated ions and using the long-range term improved the description of the activity coefficients of ChCl and water at 298.15 and 313.15 K.

3.2. VLE

Figure 3 shows the VLE in ChCl/water modeled assuming different representations of ChCl and using the binary interaction parameters obtained considering ChCl melting properties Set 1 (Figure 3a, c, and e) and Set 2 (Figure 3b, d, and f). As seen in Figure 3a and b, the ChCl representation does not influence the calculated bubble point of the mixture at a water mole fraction of 0.9292 (blue lines in Figure 3a and b). This is because the system can be considered ideal when the mole fraction of water is close to one. In contrast, when the

mole fraction of water is 0.8002 and the ChCl melting properties Set 1 are used (orange lines in Figure 3a), the associated ion representation provides the best correlation for the bubble point of the mixture, while the dissociated ion representation overestimates the bubble-point temperature of the mixture. As seen in Figure 3b, assuming ChCl as dissociated ions and using ChCl melting properties Set 2 allows for a good correlation for the bubble point of the mixture.

Figure 3c and d shows the bubble-point pressure of ChCl/water at constant temperature. As can be seen, the deviation from the experimental data increases at higher temperatures. The calculated bubble-point pressure, assuming dissociated ions representation (solid lines in Figure 3c and d) is always lower than when assuming associated ions representation (dotted and dashed lines in Figure 3c and d). The bubble-point pressure is better correlated when ChCl is assumed to be fully dissociated into ions using the ChCl melting properties Sets 1 and 2 (solid lines in Figure 3c and d).

Figure 3e,f shows the bubble-point temperature of ChCl/water at constant pressure. Similar to what is observed in bubble-point pressure modeling, assuming the dissociated ion representation predicts higher bubble-point temperatures than assuming the associated ions representation. The calculated bubble-point temperatures agree with experimental data when assuming the dissociated ions representation and using ChCl melting properties Set 1 (solid lines in Figure 3e). In contrast, the bubble-point temperature cannot be correlated when using ChCl melting properties Set 2 (Figure 3f). Moreover, the deviation from the experimental data increases as the temperature increases.

In conclusion, VLE in ChCl/water can be accurately modeled when ChCl is considered as fully dissociated ions. For instance, a strong negative deviation from ideality is needed to describe the bubble-point temperature of the mixture at high temperatures, which can be captured when assuming ChCl as dissociated ions and using ChCl melting properties Set 1. On the other hand, using ChCl melting properties Set 2 allows for describing the bubble-point of the mixture at moderate temperatures.

3.3. SLE

Figure 4 shows SLE in ChCl/water modeled by assuming different representations of ChCl and using ChCl melting properties Set 1 (Figure 4a) and Set 2 (Figure 4b). As seen in Figure 4, the liquidus lines calculated assuming ChCl as associated ions, with and without the long-range term, are similar, indicating that the long-range interaction term does not influence the calculated activity coefficients of ChCl at high salt concentrations. As seen in Figure 4a, ChCl liquidus data can be better modeled when assuming the dissociated ions representation. In contrast, the liquidus data of water and the eutectic temperature of the mixture can only be modeled when assuming ChCl as associated ions. As can be seen, no eutectic temperature can be calculated when assuming ChCl as dissociated ions, which is attributed to the significant negative deviation from ideality. This is consistent with the calculated activity coefficients of water at 298.15 and 313.15 K, assuming dissociated ions (solid lines in Figure 1a). As seen in Figure 4b, assuming ChCl as dissociated ions and using ChCl melting properties Set 2 allows for correctly modeling the complete SLE phase diagram. In conclusion, a strong negative deviation from ideality is needed to describe the SLE phase diagram of ChCl/water. Assuming ChCl as dissociated ions allows for describing the liquidus line of ChCl using either ChCl melting properties Set 1 or 2, whereas the latter better predicts the eutectic temperature of the mixture.

3.4. Intermolecular Interactions

The infinite dilution activity coefficients of components provide insight into the affinity of the solute to the solvent. Table 2 lists the infinite dilution activity coefficients of water in

Table 2. Infinite Dilution Activity Coefficients of Water and Choline Chloride (ChCl) in ChCl/Water, Calculated at 298.15 K

Approach	$\ln \gamma_{\text{water}}^{\infty}$	$\ln \gamma_{\pm}^{\infty}$	$\ln \gamma_{+}^{\text{SR},\infty}$	$\ln \gamma_{-}^{\text{SR},\infty}$
Melting Properties Set 1				
Associated ions	-4.3574	-4.7274	-	-
Associated ions no long-range	-4.5353	-5.6808	-	-
Dissociated ions	-4.0182	-2.3025	-1.9468	-4.5639
Melting Properties Set 2				
Associated ions	4.6099	-0.2256	-	-
Associated ions no long-range	4.6602	-1.1469	-	-
Dissociated ions	1.4376	0.1255	-2.9424	1.2853

ChCl and ChCl in water, calculated at 298.15 K. Because the closest approach parameter was fixed, the long-range contribution to the calculated activity coefficients is the same in all cases shown in Table 2, and the difference arises from the NRTL binary interaction parameters used to calculate the short-range contribution. As can be seen, favored interactions are predicted between ChCl and water when considering ChCl melting properties in Set 1. The calculated infinite dilution activity coefficients of water and ChCl do not change significantly when considering or neglecting the long-range term and assuming ChCl as an associated ion. This indicates that the strong negative deviation from ideality in the short-range contribution conceals the influence of the long-range interaction term ($\ln \gamma_{\pm}^{\text{SR}} = -5.6831$ and $\ln \gamma_{\pm}^{\text{LR}} = 0.9541$). Accordingly, the strong negative deviation from ideality does

not allow for describing the activity coefficients of ChCl at a low salt concentration (Figure 2a). When assuming the dissociated ions representation, the influence of the cation and anion activity coefficients on the calculated infinite dilution mean activity coefficients of ChCl can be evaluated. As can be seen, when using ChCl melting properties Set 1, the model predicts that the anion–water interactions are more favored than cation–water interactions. This is in line with several thermodynamic and molecular simulation studies that highlighted the role of the anion in determining the deviation from ideality in DES.^{23,47,52–54} Furthermore, the infinite dilution activity coefficients of water using ChCl melting properties Set 1 do not significantly change for different molecular representations of ChCl.

On the other hand, when using ChCl melting properties Set 2, unfavorable interactions are observed between water and ChCl. Moreover, ChCl shows quasi-ideal behavior in the liquid phase. The quasi-ideal behavior increases the influence of considering the long-range term on the calculated activity coefficient of ChCl. Accordingly, ChCl activity coefficients could be well described (Figure 2b). In contrast, the quasi-ideal behavior does not allow for the description of the VLE data of the mixture when assuming ChCl as associated ions. As can be seen, the model predicts that the cation–water interactions are more favored than the anion–water interactions when using ChCl melting properties Set 2. In conclusion, the activity coefficients of ChCl obtained from isopiestic measurements are primarily influenced by the long-range interaction term. On the other hand, a strong negative deviation from ideality is needed to describe VLE and SLE data, which predominantly result from the short-range contribution. Thus, the dissociated ion molecular representation better captures the nonideality of the mixture at low and high ChCl concentrations.

The partial molar excess enthalpy (\bar{h}_i^E) reflects the temperature dependence of the activity coefficients. Figure 5 shows the calculated \bar{h}_{water}^E under different representations of ChCl. As shown in Figure 5a, the binary interaction parameters obtained using ChCl melting properties Set 1 significantly underestimate \bar{h}_{water}^E . In contrast, the binary interaction parameters obtained using ChCl melting properties Set 2 slightly overestimate \bar{h}_{water}^E . These observations are consistent with the calculated VLE and SLE data. For instance, the VLE data at high temperatures can be better represented using ChCl melting properties Set 1, as this parameter set introduces a stronger temperature dependence on the water activity coefficients, although this effect may not fully reflect the actual physical behavior.

As seen in Figure 5, the inclusion of the long-range interaction term and the dissociated ions representation results in more negative values of \bar{h}_{water}^E . Nevertheless, the strong temperature dependence of activity coefficients when assuming dissociated ions and using ChCl melting properties Set 1 leads to a significant underestimation of the melting temperature of the mixture, preventing the calculation of the eutectic temperature. In conclusion, assessing the \bar{h}_{water}^E highlights the challenge of simultaneously modeling VLE and SLE data, providing critical insight into the limitations and trade-offs of modeling approaches for such systems.

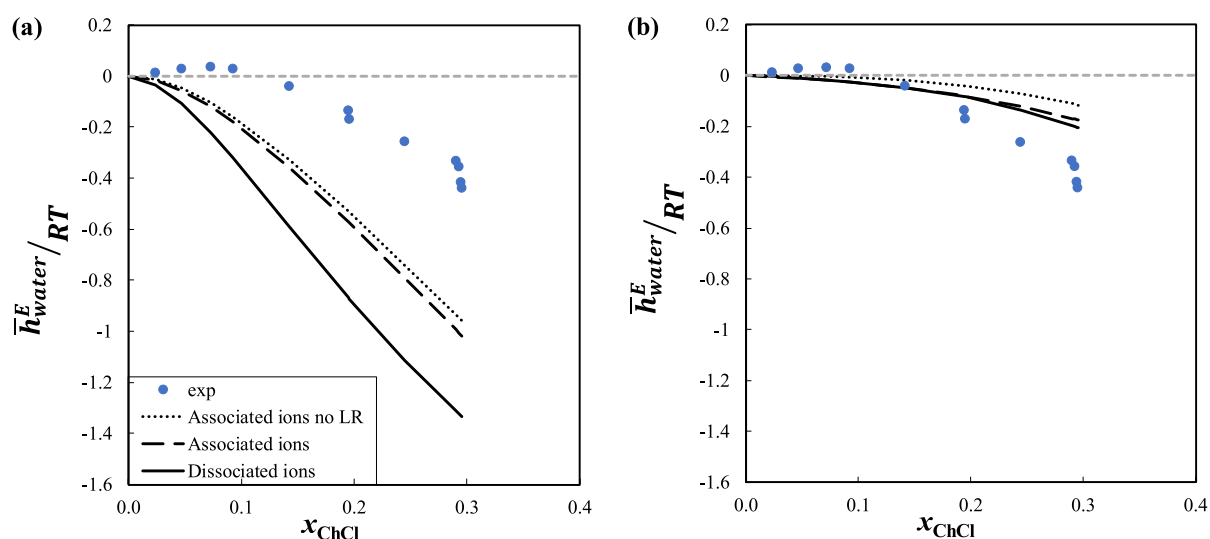


Figure 5. Partial molar excess enthalpy of water in choline chloride (ChCl)/water calculated assuming different representations of ChCl and using the binary interaction parameters obtained when considering the melting properties of ChCl reported by (a) van den Bruinhorst et al.³ or (b) Fernandez et al.⁴⁹ Experimental data were taken from⁴⁷.

4. CONCLUSIONS

This study investigates the long-range interaction term in modeling a salt-based eutectic mixture with a low melting temperature. The nonideality of the ChCl/water system was modeled considering short- and long-range interactions. The short-range interactions were modeled by using the NRTL model, and the long-range interactions were modeled by using the PDH term. The NRTL parameters were fitted to experimental VLE, SLE, and activity coefficients of components using two different ChCl melting property sets. It was found that considering ChCl as a fully dissociated ion improved the description of the activity coefficients, VLE, and SLE data. The dissociated ion representation predicts a strong negative deviation from ideality at high ChCl concentrations, which is required to correlate the VLE and SLE data. On the other hand, at low ChCl concentrations, the effect of the long-range interaction term is more dominant, which allows for reproducing the ChCl activity coefficients obtained from isopiestic measurements.

This work shows that modeling salt-based eutectic mixtures as electrolyte systems is essential to fully capture the nonideality of the mixture and to allow accurate modeling of their phase behavior. Nevertheless, several limitations were identified in this work. First, more advanced terms are needed to describe the long-range interactions in DES systems due to the strong negative deviation from ideality observed in the mixture, which might conceal the influence of the PDH term. Second, the melting enthalpy and heat capacity difference of ChCl have to be reassessed to reliably extract and analyze the ChCl activity coefficients from SLE data. Finally, modeling long-range interactions requires quality data for the density and permittivity of the components over a wide temperature range, which are challenging to obtain for most solid compounds that melt at very high temperatures.

■ ASSOCIATED CONTENT

Data Availability Statement

Data supporting the work's findings are available in the manuscript and [Supporting Information file](#).

SI Supporting Information

The Supporting Information is available free of charge at <https://pubs.acs.org/doi/10.1021/acs.iecr.5c04412>.

Debye–Hückel parameter temperature dependence, choline chloride mean ionic activity coefficients, water vapour pressure equation, NRTL interaction parameters and errors in the representation of different types of data (XLSX)

Debye–Hückel parameter of water as a function of temperature; mean activity coefficients of choline chloride in water at 298.15 K, calculated by the Pitzer–Debye–Hückel term; saturation pressure of water; NRTL binary interaction parameters obtained in this work (PDF)

■ AUTHOR INFORMATION

Corresponding Author

Simão P. Pinho – CIMO-Mountain Research Center, LA SusTEC, Instituto Politécnico de Bragança, Bragança 5300-253, Portugal; orcid.org/0000-0002-9211-857X; Phone: +351 273 303 086; Email: spinho@ipb.pt; Fax: +351 273 313 051

Authors

Ahmad Alhadid – College of Engineering and Technology, American University of the Middle East, Egaila S4200, Kuwait; orcid.org/0000-0003-1443-1517

Mirjana Minceva – Biothermodynamics, TUM School of Life Sciences, Technical University of Munich, Freising 85354, Germany; orcid.org/0000-0001-9820-7410

João A. P. Coutinho – CICECO – Aveiro Institute of Materials, Department of Chemistry, University of Aveiro, Aveiro 3810-193, Portugal; orcid.org/0000-0002-3841-743X

Complete contact information is available at: <https://pubs.acs.org/doi/10.1021/acs.iecr.5c04412>

Author Contributions

A.A.: Conceptualization, Investigation, Methodology, Formal Analysis, Data Curation, Writing – Original Draft. M.M.: Conceptualization, Formal Analysis, Resources, Writing – Review and Editing. J.A.P. C.: Conceptualization, Formal Analysis, Writing – Review and Editing. S.P.P.: Conceptualization, Investigation, Methodology, Formal Analysis, Writing – Review and Editing, Supervision.

Notes

The authors declare no competing financial interest.

ACKNOWLEDGMENTS

This work was developed within the scope of the project CIMO-Centro de Investigação de Montanha, UIDB/00690/2020 (DOI: 10.54499/UIDB/00690/2020), UIDP/00690/2020 (DOI: 10.54499/UIDP/00690/2020); and SusTEC, LA/P/0007/2020 (DOI: 10.54499/LA/P/0007/2020), and CICECO-Aveiro Institute of Materials, UIDB/50011/2020 (DOI: 10.54499/UIDB/50011/2020), UIDP/50011/2020 (DOI: 10.54499/UIDP/50011/2020) & LA/P/0006/2020 (DOI: 10.54499/LA/P/0006/2020), all financed by national funds through the FCT/MCTES (PIDDAC).

REFERENCES

- (1) Yeow, A. T. H.; Hayyan, A.; Hayyan, M.; Junaidi, M. U. M.; Saleh, J.; Basirun, W. J.; Nor, N. R. M.; Al Abdulmonem, W.; Salleh, Z. M.; Zuki, F. M.; et al. A comprehensive review on the physicochemical properties of deep eutectic solvents. *Results Chem.* **2024**, *7*, 101378.
- (2) Elhamarnah, Y.; Qiblawey, H.; Nasser, M. A review on Deep eutectic solvents as the emerging class of green solvents for membrane fabrication and separations. *J. Mol. Liq.* **2024**, *398*, 124250.
- (3) van den Bruinhorst, A.; Avila, J.; Rosenthal, M.; Pellegrino, A.; Burghammer, M.; Costa Gomes, M. Defying decomposition: The curious case of choline chloride. *Nat. Commun.* **2023**, *14* (1), 6684.
- (4) Martins, M. A. R.; Pinho, S. P.; Coutinho, J. A. P. Insights into the Nature of Eutectic and Deep Eutectic Mixtures. *J. Solution Chem.* **2019**, *48* (7), 962–982.
- (5) Alhadid, A.; Nasrallah, S.; Mokrushina, L.; Minceva, M. Design of Deep Eutectic Systems: Plastic Crystalline Materials as Constituents. *Molecules* **2022**, *27*, 6210.
- (6) Kollau, L. J. B. M.; Vis, M.; van den Bruinhorst, A.; Esteves, A. C. C.; Tuinier, R. Quantification of the liquid window of deep eutectic solvents. *Chem. Commun.* **2018**, *54* (95), 13351–13354.
- (7) Kollau, L. J. B. M.; Tuinier, R.; Verhaak, J.; den Doelder, J.; Pilot, I. A. W.; Vis, M. Design of Nonideal Eutectic Mixtures Based on Correlations with Molecular Properties. *J. Phys. Chem. B* **2020**, *124* (25), 5209–5219.
- (8) Kollau, L. J. B. M.; Vis, M.; van den Bruinhorst, A.; de With, G.; Tuinier, R. Activity modelling of the solid–liquid equilibrium of deep eutectic solvents. *Pure Appl. Chem.* **2019**, *91* (8), 1341–1349.
- (9) Wang, K.; Peng, D.; Alhadid, A.; Minceva, M. Assessment of COSMO-RS for Predicting Liquid–Liquid Equilibrium in Systems Containing Deep Eutectic Solvents. *Ind. Eng. Chem. Res.* **2024**, *63* (25), 11110–11120.
- (10) Alhadid, A.; Jandl, C.; Mokrushina, L.; Minceva, M. Nonideality and cocrystal formation in l-menthol/xlenol eutectic systems. *J. Mol. Liq.* **2022**, *367*, 120582.
- (11) Song, Z.; Wang, J.; Sundmacher, K. Evaluation of COSMO-RS for solid–liquid equilibria prediction of binary eutectic solvent systems. *Green Energy Environ.* **2021**, *6* (3), 371–379.
- (12) Song, Z.; Zhou, T.; Qi, Z.; Sundmacher, K.; Türkay, M.; Gani Elsevier, R. Computer-Aided Screening of Deep Eutectic Solvent Systems for the Associative Extraction of α -Tocopherol from Deodorizer Distillate. *Comput. Aided Chem. Eng.* **2021**, *50*, 341–346.
- (13) Peng, D.; Alhadid, A.; Minceva, M. Assessment of COSMO-SAC Predictions for Solid–Liquid Equilibrium in Binary Eutectic Systems. *Ind. Eng. Chem. Res.* **2022**, *61* (35), 13256–13264.
- (14) Abranches, D. O.; Larriba, M.; Silva, L. P.; Melle-Franco, M.; Palomar, J. F.; Pinho, S. P.; Coutinho, J. A. P. Using COSMO-RS to design choline chloride pharmaceutical eutectic solvents. *Fluid Phase Equilib.* **2019**, *497*, 71–78.
- (15) Song, Z.; Chen, J.; Qin, H.; Qi, Z.; Sundmacher, K. Extending UNIFAC models for solid-liquid equilibria prediction and design of eutectic solvent systems. *Chem. Eng. Sci.* **2023**, *281*, 119097.
- (16) Xin, K.; Roghair, I.; Gallucci, F.; van Sint Annaland, M. Total vapor pressure of hydrophobic deep eutectic solvents: Experiments and modelling. *J. Mol. Liq.* **2021**, *325*, 115227.
- (17) Wolbert, F.; Brandenbusch, C.; Sadowski, G. Selecting Excipients Forming Therapeutic Deep Eutectic Systems-A Mechanistic Approach. *Mol. Pharmaceutics* **2019**, *16* (7), 3091–3099.
- (18) Alhadid, A.; Mokrushina, L.; Minceva, M. Formation of glassy phases and polymorphism in deep eutectic solvents. *J. Mol. Liq.* **2020**, *314*, 113667.
- (19) Vilas-Boas, S. M.; Abranches, D. O.; Crespo, E. A.; Ferreira, O.; Coutinho, J. A. P.; Pinho, S. P. Experimental solubility and density studies on aqueous solutions of quaternary ammonium halides, and thermodynamic modelling for melting enthalpy estimations. *J. Mol. Liq.* **2020**, *300*, 112281.
- (20) Pontes, P. V. A.; Crespo, E. A.; Martins, M. A. R.; Silva, L. P.; Neves, C. M. S. S.; Maximo, G. J.; Hubinger, M. D.; Batista, E. A. C.; Pinho, S. P.; Coutinho, J. A. P.; et al. Measurement and PC-SAFT modeling of solid-liquid equilibrium of deep eutectic solvents of quaternary ammonium chlorides and carboxylic acids. *Fluid Phase Equilib.* **2017**, *448*, 69–80.
- (21) Crespo, E. A.; Silva, L. P.; Martins, M. A. R.; Bülow, M.; Ferreira, O.; Sadowski, G.; Held, C.; Pinho, S. P.; Coutinho, J. A. P. The Role of Polyfunctionality in the Formation of [Ch]Cl-Carboxylic Acid-Based Deep Eutectic Solvents. *Ind. Eng. Chem. Res.* **2018**, *57* (32), 11195–11209.
- (22) Crespo, E. A.; Silva, L. P.; Martins, M. A. R.; Fernandez, L.; Ortega, J.; Ferreira, O.; Sadowski, G.; Held, C.; Pinho, S. P.; Coutinho, J. A. P. Characterization and Modeling of the Liquid Phase of Deep Eutectic Solvents Based on Fatty Acids/Alcohols and Choline Chloride. *Ind. Eng. Chem. Res.* **2017**, *56* (42), 12192–12202.
- (23) van den Bruinhorst, A.; Kollau, L. J. B. M.; Vis, M.; Hendrix, M. M. R. M.; Meuldijk, J.; Tuinier, R.; Esteves, A. C. C. From a eutectic mixture to a deep eutectic system via anion selection: Glutaric acid + tetraethylammonium halides. *J. Chem. Phys.* **2021**, *155* (1), 014502.
- (24) González de Castilla, A.; Bittner, J. P.; Müller, S.; Jakobtorweihen, S.; Smirnova, I. Thermodynamic and Transport Properties Modeling of Deep Eutectic Solvents: A Review on gE-Models, Equations of State, and Molecular Dynamics. *J. Chem. Eng. Data* **2020**, *65* (3), 943–967.
- (25) Crespo, E. A.; Silva, L. P.; Lloret, J. O.; Carvalho, P. J.; Vega, L. F.; Llovel, F.; Coutinho, J. A. P. A methodology to parameterize SAFT-type equations of state for solid precursors of deep eutectic solvents: The example of cholinium chloride. *Phys. Chem. Chem. Phys.* **2019**, *21* (27), 15046–15061.
- (26) Gholami, S.; Roosta, A. Bubble point of aqueous mixtures of sugar-based deep eutectic solvents and their individual components: Experimental study and modeling. *J. Mol. Liq.* **2019**, *296*, 111876.
- (27) Moghimi, M.; Roosta, A.; Hekayati, J.; Rezaei, N. Estimating VLE behavior from SLE data in aqueous mixtures of choline chloride-sorbitol deep eutectic solvents: Experimental investigation and thermodynamic modeling using the e-NRTL model. *J. Mol. Liq.* **2023**, *371*, 121126.
- (28) Prausnitz, J. M.; Lichtenthaler, R. N.; Azevedo, E. G. D. *Molecular Thermodynamics of Fluid-Phase Equilibria*; Prentice Hall PTR, 1999.
- (29) Pitzer, K. S. E. From dilute solutions to fused salts. *J. Am. Chem. Soc.* **1980**, *102* (9), 2902–2906.

- (30) Chang, C.-K.; Lin, S.-T. Extended Pitzer–Debye–Hückel Model for Long-Range Interactions in Ionic Liquids. *J. Chem. Eng. Data* **2020**, *65* (3), 1019–1027.
- (31) Marques, H.; González de Castilla, A.; Müller, S.; Smirnova, I. Impact of extended long-range electrostatics on the correlation of liquid-liquid equilibria in aqueous ionic liquid systems. *Fluid Phase Equilib.* **2023**, *569*, 113765.
- (32) González de Castilla, A.; Müller, S.; Smirnova, I. On the analogy between the restricted primitive model and capacitor circuits. Part II: A generalized Gibbs-Duhem consistent extension of the Pitzer-Debye-Hückel term with corrections for low and variable relative permittivity. *J. Mol. Liq.* **2022**, *360*, 119398.
- (33) Lee, B.-S.; Lin, S.-T. A Priori Prediction of Dissociation Phenomena and Phase Behaviors of Ionic Liquids. *Ind. Eng. Chem. Res.* **2015**, *54* (36), 9005–9012.
- (34) Ma, C.; Laaksonen, A.; Liu, C.; Lu, X.; Ji, X. The peculiar effect of water on ionic liquids and deep eutectic solvents. *Chem. Soc. Rev.* **2018**, *47* (23), 8685–8720.
- (35) Lobo Ferreira, A. I. M. C.; Vilas-Boas, S. M.; Silva, R. M. A.; Martins, M. A. R.; Abranches, D. O.; Soares-Santos, P. C. R.; Almeida Paz, F. A.; Ferreira, O.; Pinho, S. P.; Santos, L. M. N. B. F.; et al. Extensive characterization of choline chloride and its solid–liquid equilibrium with water. *Phys. Chem. Chem. Phys.* **2022**, *24* (24), 14886–14897.
- (36) Mangiacapre, E.; Castiglione, F.; D’Aristotile, M.; Di Lisio, V.; Triolo, A.; Russina, O. Choline chloride-water mixtures as new generation of green solvents: A comprehensive physico-chemical study. *J. Mol. Liq.* **2023**, *383*, 122120.
- (37) Francisco, M.; van den Bruinhorst, A.; Kroon, M. C. Low-Transition-Temperature Mixtures (LTTMs): A New Generation of Designer Solvents. *Angew. Chem., Int. Ed.* **2013**, *52* (11), 3074–3085.
- (38) Catenaccio, A.; Daruich, Y.; Magallanes, C. Temperature dependence of the permittivity of water. *Chem. Phys. Lett.* **2003**, *367* (5), 669–671.
- (39) Clarke, E. C. W.; Glew, D. N. Evaluation of Debye–Hückel limiting slopes for water between 0 and 150°C. *J. Chem. Soc., Faraday Trans.1* **1980**, *76*, 1911–1916.
- (40) Fleming, R. S. The activity coefficients of aqueous solutions of choline chloride at 25°C. *J. Chem. Soc.* **1961**, 3100–3102.
- (41) Macaskill, J. B.; Mohan, M. S.; Bates, R. G. Activity coefficients and osmotic coefficients in aqueous solutions of choline chloride at 25°C. *Anal. Chem.* **1977**, *49* (2), 209–212.
- (42) Boyd, G. E.; Schwarz, A.; Lindenbaum, S. Structural Effects on the Osmotic and Activity Coefficients of the Quaternary Ammonium Halides in Aqueous Solutions at 25°C. *J. Phys. Chem.* **1966**, *70* (3), 821–825.
- (43) Khan, I.; Kurnia, K. A.; Sintra, T. E.; Saraiva, J. A.; Pinho, S. P.; Coutinho, J. A. P. Assessing the activity coefficients of water in cholinium-based ionic liquids: Experimental measurements and COSMO-RS modeling. *Fluid Phase Equilib.* **2014**, *361*, 16–22.
- (44) Velho, P.; Sousa, E.; Macedo, E. A. Binary aqueous solutions of choline salts: Determination and modelling of liquid density (298.15 or 313.15 K) and Vapour Pressure Osmometry (313.15 K). *Fluid Phase Equilib.* **2025**, *587*, 114197.
- (45) Francisco, M.; González, A. S. B.; García de Dios, S. L.; Weggemans, W.; Kroon, M. C. Comparison of a low transition temperature mixture (LTTM) formed by lactic acid and choline chloride with choline lactate ionic liquid and the choline chloride salt: Physical properties and vapour–liquid equilibria of mixtures containing water and ethanol. *RSC Adv.* **2013**, *3* (45), 23553–23561.
- (46) Carvalho, P. J.; Khan, I.; Morais, A.; Granjo, J. F. O.; Oliveira, N. M. C.; Santos, L. M. N. B. F.; Coutinho, J. A. P. A new microbullimometer for the measurement of the vapor–liquid equilibrium of ionic liquid systems. *Fluid Phase Equilib.* **2013**, *354*, 156–165.
- (47) van den Bruinhorst, A.; Corsini, C.; Depraetère, G.; Cam, N.; Pádua, A.; Costa Gomes, M. Deep eutectic solvents on a tightrope: Balancing the entropy and enthalpy of mixing. *Faraday Discuss* **2024**, *253*, 273–288.
- (48) Matsunaga, N.; Nagashima, A. Saturation vapor pressure and critical constants of H₂O, D₂O, T₂O, and their isotopic mixtures. *Int. J. Thermophys.* **1987**, *8* (6), 681–694.
- (49) Fernandez, L.; Silva, L. P.; Martins, M. A. R.; Ferreira, O.; Ortega, J.; Pinho, S. P.; Coutinho, J. A. P. Indirect assessment of the fusion properties of choline chloride from solid-liquid equilibria data. *Fluid Phase Equilib.* **2017**, *448*, 9–14.
- (50) Pinho, S. P.; Macedo, E. A. Representation of salt solubility in mixed solvents: A comparison of thermodynamic models. *Fluid Phase Equilib.* **1996**, *116* (1), 209–216.
- (51) Bazyleva, A.; Acree, W. E.; Diky, V.; Hefter, G. T.; Jacquemin, J.; Magalhães, M. C. F.; Magee, J. W.; Nordstrom, D. K.; O’Connell, J. P.; Olson, J. D.; et al. Reference materials for phase equilibrium studies. 2. Solid–liquid equilibria (IUPAC Technical Report). *Pure Appl. Chem.* **2022**, *94* (11–12), 1225–1247.
- (52) Alhadid, A.; Jandl, C.; Nasrallah, S.; Kronawitter, S. M.; Mokrushina, L.; Kieslich, G.; Minceva, M. Estimating the nonideality of eutectic systems containing thermally unstable substances. *J. Chem. Phys.* **2023**, *159* (9), 094503.
- (53) Martins, M. A. R.; Abranches, D. O.; Silva, L. P.; Pinho, S. P.; Coutinho, J. A. P. Insights into the Chloride versus Bromide Effect on the Formation of Urea-Quaternary Ammonium Eutectic Solvents. *Ind. Eng. Chem. Res.* **2022**, *61* (32), 11988–11995.
- (54) Sarkar, S.; Maity, A.; Chakrabarti, R. In Silico Elucidation of Molecular Picture of Water–Choline Chloride Mixture. *J. Phys. Chem. B* **2021**, *125* (48), 13212–13228.



CAS INSIGHTS™

EXPLORE THE INNOVATIONS SHAPING TOMORROW

Discover the latest scientific research and trends with CAS Insights. Subscribe for email updates on new articles, reports, and webinars at the intersection of science and innovation.

[Subscribe today](#)

CAS
A division of the
American Chemical Society